Multiaxial Deformations of End-Linked Poly(dimethylsiloxane) Networks. 1. Phenomenological Approach to Strain Energy Density Function

Takanobu Kawamura, Kenji Urayama,* and Shinzo Kohjiya

Institute for Chemical Research, Kyoto University, Uji, Kyoto-fu 611-0011, Japan

Received December 20, 2000; Revised Manuscript Received June 20, 2001

ABSTRACT: The phenomenological strain energy density function (W) for the elastomeric networks of end-linked poly(dimethylsiloxane) (PDMS) has been investigated as a function of the first and second invariants I_1 and I_2 of the Green's deformation tensor on the basis of the quasi-equilibrium stress−strain relationships of general biaxial deformations varying independently each of two principal strains. The I_i dependence of $\partial W/\partial I_j$ ($i,j = 1,2$) was obtained from the biaxial stress−strain data using the Rivlin−Saunders method. In the 3-dimensional plots of $\partial W/\partial I_i$ ($i = 1,2$) against both the $(I_1 - 3)$- and $(I_2 - 3)$-axes, the data points of each derivative at large deformations appear to fall on a plane inclining against the (I_1,I_2) plane, which suggests that both the derivatives linearly depend on each of I_1 and I_2. The formula of W is reasonably deduced from such linear dependence of $\partial W/\partial I_i$ on I_j ($i,j = 1,2$) as $W = C_{10}(I_1 - 3) + C_{01}(I_2 - 3) + C_{11}(I_1 - 3)(I_2 - 3) + C_{20}(I_1 - 3)^2 + C_{02}(I_2 - 3)^2$. Each of the numerical coefficients C_{ij} is assigned to each of the intercepts at $I_1 = I_2 = 3$ and the gradients of the two fitted planes in the (I_1, I_2, $\partial W/\partial I_i$) plots. The estimated W satisfactorily reproduces not only the original biaxial stress−strain data but also the data of uniaxial, equibiaxial elongation, and uniaxial compression none of which were used for the original estimation of W. It is also demonstrated that the familiar Mooney−Rivlin type of W composed of only two linear terms of each of I_1 and I_2 does not even qualitatively reproduce the biaxial stress−strain data.

Introduction

The strain energy density function (W) of cross-linked amorphous polymer (elastomer) has been both theoretically and experimentally investigated for the comprehensive understanding of rubber elasticity.[1,2] The function W corresponds to the elastic free energy governing the stress−strain relationship of elastomer under general deformations. The investigation of W is very significant from viewpoint of not only academic interests in rubber elasticity but also practical applications of elastomer. When the functional form of W is known, one can evaluate the 3-dimensional stresses (strains) under any given 3-dimensional strains (stresses). The finite elemental analysis for the designs of rubber engineering components demands proper selection of W with appropriate material parameters.[3] Many types of phenomenological W have been proposed to describe the stress−strain behavior of real elastomers, and the proposed formulas are summarized in some reviews.[1,3−5]

To deduce experimentally the phenomenological W of an incompressible material like elastomer, it is important to collect as many combinations of 2-dimensional stress and strain as possible. Uniaxial deformation has often been employed for the estimation of W due to the experimental simplicity. However, uniaxial deformation gives too restricted a basis to deduce the true form of W, because it is only a particular case among all accessible deformations. The estimation of W relying on only uniaxial deformation often results in an incorrect W which does not reproduce elastic response under other deformations. As Rivlin and Saunders[6] clearly suggested, a powerful method for the estimation of W is the biaxial elongation experiment to measure the two sets of stresses and strains in two orthogonal stretching directions. Actually it is possible to achieve all accessible pure homogeneous strains for an incompressible material by changing independently each of the two principal strains (general biaxial strains).[1,7] Treloar et al.,[8−10] Landel et al.,[11−13] Becker,[14] James et al.,[15] and Kawabata et al.[16,17] performed the general biaxial stretching experiments for some rubber vulcanizates, and some of them proposed a phenomenological W on the basis of their own experimental data.

In the present study, the quasi-equilibrium stress−strain relationships of end-linked poly(dimethylsiloxane) (PDMS) networks have been investigated by the general biaxial stretching experiments which cover the whole range of pure homogeneous deformations from uniaxial stretching to equibiaxial stretching. The very low crystalline melting temperature (ca. −40 °C) of PDMS[18,19] is an advantage, since one can avoid the complications from strain-induced crystallization which is observed in natural rubbers. An interesting point is that the behavior of PDMS networks composed of siloxane backbone can be expected to be fundamentally different from that of the hydrocarbon networks. The PDMS networks were prepared by end-linking end-reactive precursor PDMS with tetrafunctional cross-linker. End-linked polymer network has often been used as a well-characterized network in the studies aiming at the molecular interpretation of rubber elasticity, because in principle the distance between topologically neighboring cross-links and the functionality of cross-links can be controlled by the size of end-reactive precursor polymer and the functionality of cross-linker, respectively.[20−25] Most of the earlier studies on rubber elasticity of end-linked networks have been performed by uniaxial deformation except for one study[22] using equibiaxial elongation achieved by inflation. However, general biaxial deformation behavior of an end-linked network has not yet

* To whom correspondence should be addressed: E-mail: urayama@scl.kyoto-u.ac.jp.

10.1021/ma002165y CCC: $20.00
Published on Web 10/09/2001

been investigated to our knowledge. The elastomer samples employed in all the earlier general biaxial deformation experiments were the "randomly" cross-linked networks whose molecular characteristics such as network chain length and cross-linking density are much more obscure relative to the end-linked networks. The general biaxial deformation experiment of an end-linked network is also very important for the purpose of the rigorous experimental tests of molecular theories for rubber elasticity. This subject is treated in our subsequent paper.[26] The main aim in the present paper is to estimate the phenomenological W reproducing the stress−strain relations under general deformations of the end-linked PDMS networks. First, the formula of W as a function of the two invariants of deformation tensor I_1 and I_2 is deduced from the I_1 and I_2 dependence of $\partial W/\partial I_i$ ($i = 1,2$) which is obtained from the stress−strain data of general biaxial elongation. Second, the estimated W is tested by uniaxial, equibiaxial elongation and uniaxial compression, whose stress−strain data are not used for the original deduction of W. Finally, it is once again shown that the Mooney−Rivlin function[27,28] of W, which is the origin of the familiar Mooney−Rivlin plot for uniaxial elongation data, has poor reproducibility for the real stress−strain behavior.

Theoretical Background

The strain energy density function W represents the elastic free energy stored in a homogeneous, isotropic and elastic material when it deforms. The function W for incompressible material is customarily expressed using the two invariants of the Green's deformation tensor I_i ($i = 1,2$) as two independent variables.

$$W = W(I_1, I_2) \tag{1}$$

$$I_1 = \lambda_1^2 + \lambda_2^2 + \lambda_3^2 \tag{2}$$

$$I_2 = \lambda_1^2\lambda_2^2 + \lambda_2^2\lambda_3^2 + \lambda_3^2\lambda_1^2 \tag{3}$$

where λ_i ($i = 1,2,3$) is the principal ratio in each of three principal axes. The third invariant I_3 ($=\lambda_1^2\lambda_2^2\lambda_3^2$) equals one for incompressible material. The phenomenological expression of W may be given by a polynominal function of $(I_1 - 3)$ and $(I_2 - 3)$:[27]

$$W(I_1,I_2) = \sum_{i,j=0}^{\infty} C_{ij}(I_1 - 3)^i(I_2 - 3)^j \tag{4}$$

where $(I_1 - 3)$ and $(I_2 - 3)$ are chosen instead of I_1 and I_2, respectively, and C_{00}=0 in order that W vanish automatically at zero strain ($I_1 = I_2 = 3$). The main aim here is *to select an appropriate set of terms as well as to assign values to the coefficients so that W can reproduce the stress−strain behavior of a material under general deformations.*

The derivatives $\partial W/\partial I_1$ and $\partial W/\partial I_2$ are related with the principal stresses σ_i ($i = 1,2$) under biaxial elongation in the 1 and 2 directions with $\sigma_3 = 0$ as follows.[6]

$$\frac{\partial W}{\partial I_1} = \frac{1}{2(\lambda_1^2 - \lambda_2^2)}\left[\frac{\lambda_1^3\sigma_1}{\lambda_1^2 - (\lambda_1\lambda_2)^{-2}} - \frac{\lambda_2^3\sigma_2}{\lambda_2^2 - (\lambda_1\lambda_2)^{-2}}\right] \tag{5}$$

$$\frac{\partial W}{\partial I_2} = \frac{-1}{2(\lambda_1^2 - \lambda_2^2)}\left[\frac{\lambda_1\sigma_1}{\lambda_1^2 - (\lambda_1\lambda_2)^{-2}} - \frac{\lambda_2\sigma_2}{\lambda_2^2 - (\lambda_1\lambda_2)^{-2}}\right] \tag{6}$$

where $\lambda_3 = 1/(\lambda_1\lambda_2)$ is used. The stress σ_i is the nominal stress, i.e., the force per unit area in the underformed state. The variations of $\partial W/\partial I_i$ on I_j ($i,j = 1,2$) are obtained from the biaxial stress−strain data (σ_1, σ_2)−(λ_1, λ_2) under various sets of λ_1 and λ_2 using eqs 2, 3, 5, and 6. It should be pointed out that eqs 5 and 6 are undefined for the two limiting deformation conditions, uniaxial ($\lambda_2 = \lambda_1^{-1/2}$, $\sigma_2 = \sigma_3 = 0$) and equibiaxial ($\lambda_1 = \lambda_2$, $\sigma_1 = \sigma_2$) stretching. Therefore, the data of the biaxial deformations of $\lambda_1 \neq \lambda_2$ are used for the calculation of $\partial W/\partial I_i$. Thus the general biaxial deformation experiment provides the dependence of $\partial W/\partial I_i$ on I_j ($i,j = 1,2$) which is a basis for deducing the functional form of $W(I_1,I_2)$.

In the present study, we concentrate on the determination of the Mooney-type W function (eq 4) using the usual invariants as independent variables. Some earlier studies[11−13] employed another phenomenological approach on the basis of the so-called Valanis−Landel hypothesis, and they did not use the Rivlin−Saunders (RS) approach to describe their results. These and any other non-RS type of treatment, which do not consider the results in terms of a general form of W, are not being considered here.

Experimental Section

Sample Preparation. Two PDMS network samples were prepared by end-linking reaction hydrosilylation between vinyl-terminated precursor PDMS and tetrakisdimethylsiloxysilane (tetrafunctional cross-linker) with or without solvent, respectively. The number- and weight-average molecular weights (M_n and M_w, respectively) of the precursor PDMS were evaluated to be 46 600 and 89 500, respectively, by gel permeation chromatography (GPC). The GPC measurement with the Shim-pack GPC80MC column was made at 54 °C using chloroform as solvent under the flow rate of 1.0 mL/min. Under this condition, molecular weight of PDMS is acquired from an elution−time curve for standard poly(styrene) samples without any further calculations.[29] The precursor chains used here are well entangled before cross-links are introduced, because the molecular mass is much larger than M_c = 16 600,[30] where M_c is the critical molecular mass to form entanglement couplings in un-crosslinked PDMS melt. The two PDMS networks were prepared from the melt and the concentrated (70 wt %) solution of PDMS, respectively. Trimethyl-terminated oligo(dimethylsiloxane) with $M_n = 3000$ was employed as a nonvolatile solvent. A platinum chloric acid dissolved in propanol (Spier's catalyst) was used as catalyst for hydrosilylation. The molar ratio of silane hydrogen in the cross-linker to vinyl group in the precursor PDMS (r) was 1.3 for the two networks which was chosen by the optimization after Patel et al. method[23] on the basis of the r dependence of the degree of equilibrium swelling.

The mixtures of the precursor PDMS, cross-linker, and catalyst (and solvent) were poured into a glass cylindrical tube with 6 mm diameter and a rectangular Teflon mold for the sample preparations for the measurements of the Poisson's ratio and biaxial elongation, respectively. The cross-linking reactions were carried out at 75 °C for 72 h.

The fractions of unreacted reactants (w_{sol}) were evaluated to be 8.76 wt % for the melt-end-linked sample and 7.50 wt % (excluding 30 wt % of oligomer solvent) for the sample prepared from 70 wt % solution by extraction measurements in toluene.

Poisson's Ratio. The Poisson's ratio of the PDMS network was evaluated from the dimension changes of uniaxially elongated cylindrical sample in both the elongation and its perpendicular directions.[31,32] The cylindrical samples whose both ends were clamped were uniaxially stepwise elongated up to a certain length, and the sizes in the two directions were measured under each elongation. The gel size in the direction perpendicular to elongation (i.e., diameter of the cylindrical sample) was measured by laser scanning micrometer LS-5040 (Kyence Co.) with an accuracy of 1 micron. The elongation ratios were determined from the distance between two markers on the sample surface, measured on the enlarged photographs of the stretched sample.

Biaxial Elongation. The biaxial elongation measurements were carried out with the biaxial stretching instrument BISS-0404 (Iwamoto Seisakusyo Co.). The mechanisms for sample-fixation, -elongation and load-detection of the instrument are essentially similar to those of the biaxial extension equipment developed by Kawabata et al..[17] The details are referred to ref 17. The specimen of a square sheet of ca. 4 cm widths and 0.5 mm thickness is clamped by four chucks at each of its four sides. The specimen is biaxially stretched in two orthogonal directions under two independently controlled strains. The clamps are mounted on roller bearings so that they can move freely along the force detecting bars according to applied deformation of the orthogonal direction. The tensile forces along the two directions are detected by two independent force-detection systems. The elongation ratio of the specimen in each direction was obtained by measuring the distance between two markings on the sample surface. The apparatus is completely covered by a temperature-controllable box. The measurements were made at 40 °C, controlled with an accuracy of better than 1 °C.

To eliminate undesirable initial relaxation components such as surface effect, the following preliminary stabilizing treatment was made prior to the collection of biaxial force−strain data: The samples were equibiaxially stretched up to a maximum elongation ratio (λ_{max}) and subsequently the applied strains were completely released. This cycle was repeated several times. After this pretreatment, in the beginning of the collection of biaxial force−strain data, the sample was equibiaxially elongated up to the λ_{max} which was 1.6 and 1.9 for the melt- and solution-end-linked networks, respectively. It was observed in preliminary experiments that equibiaxial strains beyond the λ_{max} brought about rupture. Careful optimizations were made for the sample thickness as well as the sample fixation by chucks, with the result that the rupture observed was not a premature one due to the inhomogeneity in the state of strain in the vicinity of the clamped edges (i.e., the rupture started not around the edges but in the central part of the samples). The force−strain measurements at a series of the biaxial strains of $\lambda_1 = \lambda_{max}$ and $\lambda_2 < \lambda_{max}$ were made after that at $\lambda_1 = \lambda_2 = \lambda_{max}$: The stretching in one direction (λ_2) was stepwise reduced to a given value, while that in other direction (λ_1) was fixed. After all the measurements at $\lambda_1 = \lambda_{max}$ were finished, the specimen was equibiaxially stretched to second maximum λ. The force−strain measurements under various sets of biaxial strains were conducted by repeating this procedure. The forces and strains were measured an hour after the sample was deformed in order to obtain the quasi-equilibrium ones in which time effect is sufficiently eliminated. In general, the forces reached almost equilibrium values 30 min after deformation. No appreciable effect of deformation−hysteresis on the quasi-equilibrium force−strain relations was observed; that is, there was no recognizable difference among the two sets of quasi-equilibrium biaxial forces at same biaxial strains, independently obtained through different deformation-path histories.

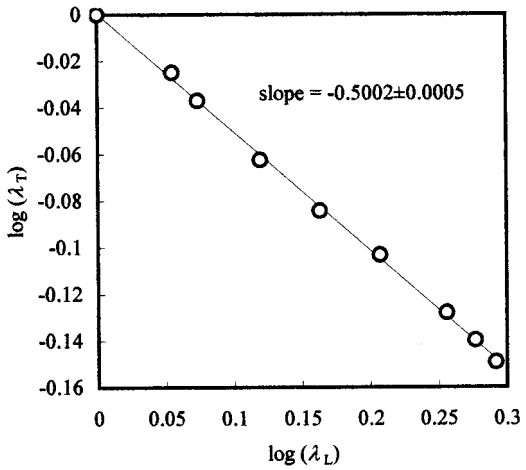

Figure 1. Double logarithmic plot of λ_L vs λ_T for the melt-end-linked PDMS network where λ_L and λ_T are the principal ratios in uniaxial elongation and its perpendicular direction, respectively. The slope was obtained by the least-squares method.

Uniaxial-Elongation and Compression. Uniaxial-elongation and compression measurements were performed with DVE-V4 (Reoroji Co.) at 40 °C. A rectangular strip of ca. 1 cm width and ca. 4 cm length, and a columnar disk of ca. 1 cm diameter, both of which were cut out from the sheet specimens used for biaxial elongation measurement, were employed for uniaxial-elongation and compression experiments, respectively. For compression measurement, the 12 pieces of the columnar disk were stacked up so that the total thickness was ca. 6 mm. The quasi-equilibrium force under each strain was measured half an hour after the sample was deformed since no appreciable further relaxation of force was observed 20 min after deformation.

Results and Discussion

Poisson's Ratio. In case of uniaxial elongation, a generalized definition of Poisson's ratio (μ) extended to large deformation is given by[31,32]

$$\lambda_T = \lambda_L^{-\mu} \tag{7}$$

where λ_L and λ_T is the principal ratio in elongation and its perpendicular directions, respectively. Figure 1 shows the double logarithmic plots of λ_T vs λ_L for the melt-end-linked network. It can be seen that all the data points fall on a straight line over the whole λ range examined here. The linear relation suggests that μ is independent of elongation ratio, and the value of μ is obtained from the slope. The estimated value of $\mu = 0.5002 \pm 0.0005$, in which experimental error in measuring the sizes was considered, is very close to 1/2 as in the case of other rubber vulcanizates.[33] The value of $\mu \sim 1/2$ suggests that incompressibility is reasonably well assumed for the rubbery samples used here.

Estimation of *W* from Stress−Strain Relation of Biaxial Elongation of $\lambda_1 \neq \lambda_2$. Parts a and b of Figure

2 show the λ_2 dependence of σ_1 and σ_2 obtained from biaxial elongation experiment for the network prepared from 70 wt % solution, respectively, together with the data of uniaxial elongation. The subscripts 1 and 2 represent the directions of larger and smaller applied strains, respectively. The dashed lines are the guide lines for the eyes showing the data at same λ_1. The triangle and rectangular symbols in the most left and right sides in each figure stand for the data of uniaxial ($\lambda_2 = \lambda_1^{-1/2}$ and $\sigma_2 = 0$) and equibiaxial ($\lambda_1 = \lambda_2$) elongation, respectively. The vertical solid line corresponds to strip-biaxial (pure shear) deformation ($\lambda_2 = 1$).

The stress−strain data of biaxial deformations of $\lambda_1 \neq \lambda_2$ were converted into the I_i dependence of $\partial W/\partial I_j$ ($i,j = 1,2$) using eqs 2, 3, 5, and 6. In the earlier studies[6,8−10,14−17] on biaxial elongation of some elastomers, the plots of $\partial W/\partial I_i$ ($i = 1,2$) vs either I_1 or I_2 have been conventionally used due to their simplicity for the data analysis. However, on the basis of the fact that each derivative is a function of two independent variables I_1 and I_2, to plot 3-dimensionally each derivative against both the I_1- and I_2-axes is more direct and helpful to estimate the functions $\partial W/\partial I_i(I_1,I_2)$. Figures 3 and 4 show the 3-dimensional plots of $\partial W/\partial I_1$ and $\partial W/\partial I_2$ against both the $(I_1 - 3)$- and $(I_2 - 3)$-axes for the networks prepared from melt and 70 wt % solution, respectively. For both the networks, the data points of each derivative except for the small strain region of $I_1,I_2 < 3.2$ appear to be on a plane inclining against the (I_1, I_2) plane. The behavior of the derivatives at the small deformations will be mentioned later, and the focus here is given to the large deformation region of $I_1,I_2 > 3.2$. The dependence of each derivative on I_1 and I_2 being approximated by a plane implies that the W is expressed by the expansion of eq 4 up to second order of $(I_1 - 3)$ and $(I_2 - 3)$ but with C_{00}, C_{12}, C_{21}, and $C_{22} = 0$ as

$$W = \sum_{i,j=0}^{2} C_{ij}(I_1 - 3)^i(I_2 - 3)^j \quad (\text{with } C_{00}, C_{12}, C_{21}, C_{22} = 0)$$

$$= C_{10}(I_1 - 3) + C_{01}(I_2 - 3) + C_{11}(I_1 - 3)(I_2 - 3) + C_{20}(I_1 - 3)^2 + C_{02}(I_2 - 3)^2 \quad (8)$$

because each derivative of W of eq 8 is a linear function of each of $(I_1 - 3)$ and $(I_2 - 3)$ in the following.

$$\frac{\partial W}{\partial I_1} = C_{10} + C_{11}(I_2 - 3) + 2C_{20}(I_1 - 3) \quad (9)$$

$$\frac{\partial W}{\partial I_2} = C_{01} + C_{11}(I_1 - 3) + 2C_{02}(I_2 - 3) \quad (10)$$

It is to be noted that the numerical coefficient of the term $(I_2 - 3)$ in eq 9 is common to that of the term $(I_1 - 3)$ in eq 10 since both the terms originate from the cross-term $C_{11}(I_1 - 3)(I_2 - 3)$ in eq 8. Under this restriction of C_{11}, the planes were successfully fitted to the experimental data of both $\partial W/\partial I_1$ and $\partial W/\partial I_2$ for the two networks, as shown in Figures 3 and 4. The numerical coefficients in eqs 9 and 10 obtained for the two samples are listed in Table 1. It should be emphasized that each of the five coefficients in eqs 9 and 10 is uniquely determined by the present analysis because each coefficient is assigned to each of the intercepts at

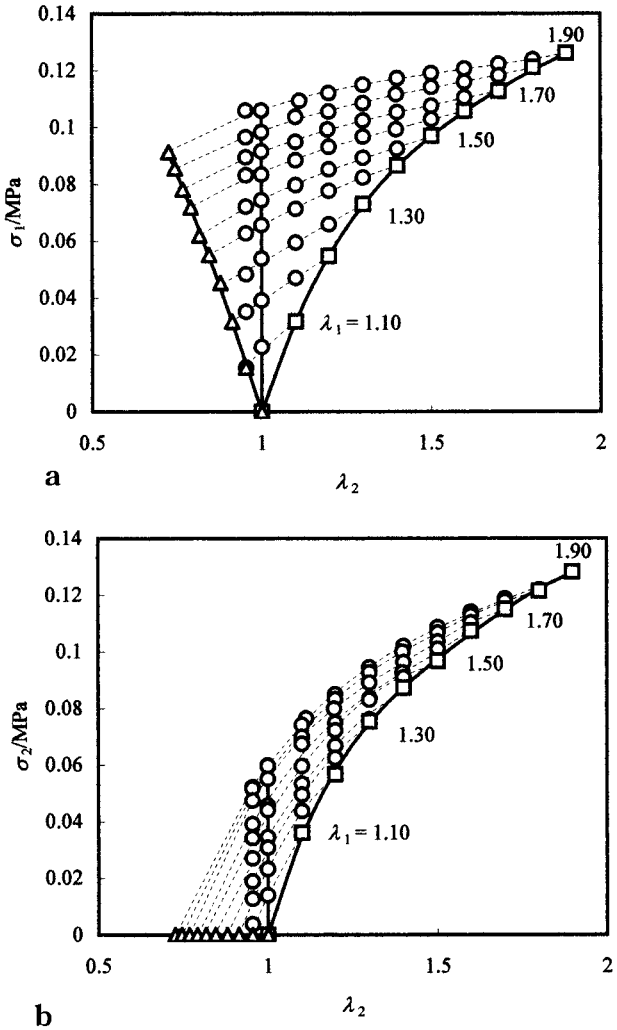

Figure 2. Principal stress (a) σ_1 and (b) σ_2 as a function of λ_2 for the end-linked PDMS network prepared from 70 wt % solution. The dashed lines are the guide lines for eyes showing the data at same λ_1. The triangular and rectangular symbols stand for the data of uniaxial and equibiaxial elongation, respectively. The vertical solid line corresponds to strip-biaxial (pure shear) deformation.

$I_1 = I_2 = 3$ or the gradients of the two planes. Thus the present analysis provides unique appropriate set of C_{ij}. A detailed discussion about the values of C_{ij} will be given in a later section.

The behavior of $\partial W/\partial I_i$ at the small deformations of $I_1,I_2 < 3.2$ seems to be complicated in contrast to the relatively simple behavior at the larger deformations. It can be seen for the melt-end-linked network that with decreasing strain, $\partial W/\partial I_1$ has the tendency to increase, while $\partial W/\partial I_2$ tends to decrease and become negative. Such small deformation behavior of the derivatives for the melt-end-linked PDMS network is qualitatively similar to the results of the biaxial experiments of some rubber vulcanizates[16,17,34] and polyurethane elastomers.[11,35] On the other hand, each of $\partial W/\partial I_i$ at the small deformations for the solution-end-linked network shows a tendency opposite to that for the melt-end-linked network. This puzzling discrepancy appears to suggest the necessity to investigate further the universality of small deformation behavior of $\partial W/\partial I_i$ for general elastomers. It is also to be noted that a small amount of error in the raw stress−strain data at small deformations causes magnified errors in the calculated values

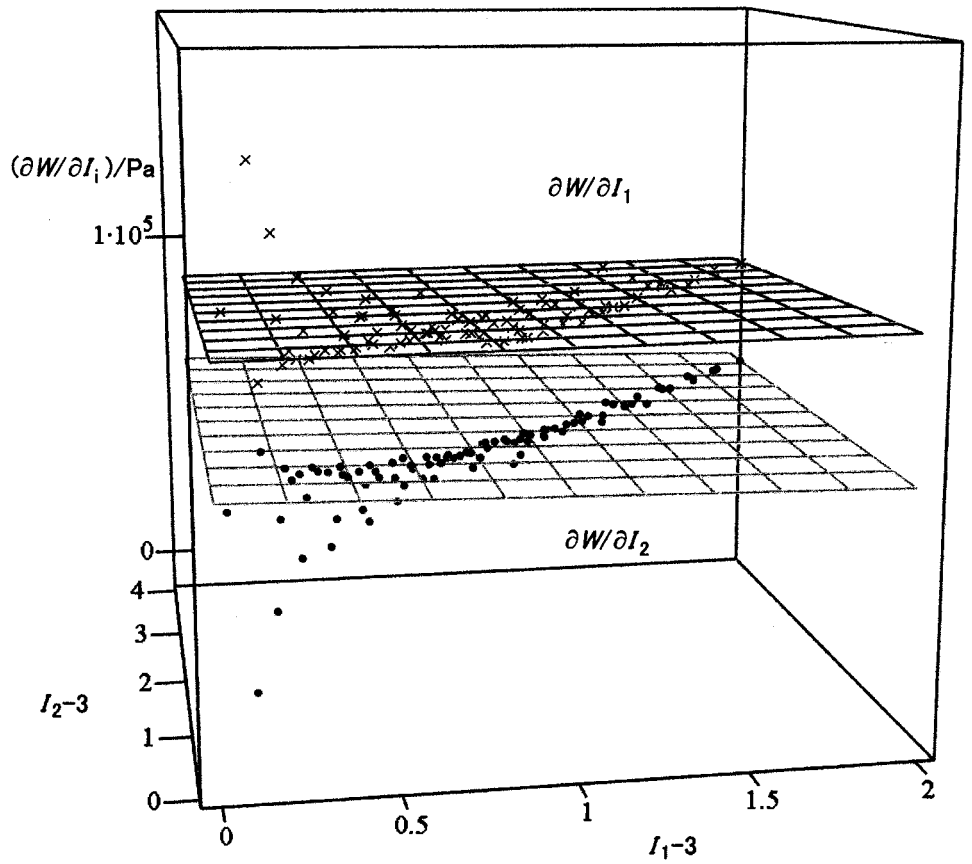

Figure 3. Derivatives $\partial W/\partial I_1$ and $\partial W/\partial I_2$ as a function of $(I_1 - 3)$ and $(I_2 - 3)$ for the melt-end-linked PDMS network. The upper and lower planes correspond to eqs 9 and 10 with C_{ij} in Table 1, respectively.

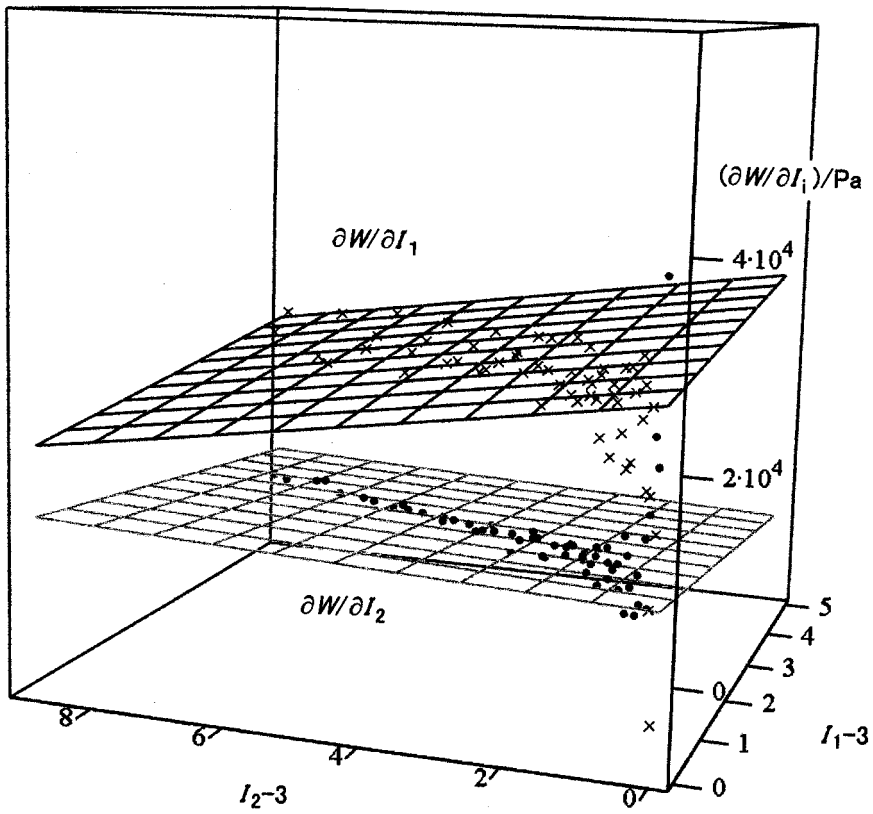

Figure 4. Derivatives $\partial W/\partial I_1$ and $\partial W/\partial I_2$ as a function of $(I_1 - 3)$ and $(I_2 - 3)$ for the end-linked PDMS network prepared from 70 wt % solution. The upper and lower planes correspond to eqs 9 and 10 with C_{ij} in Table 1, respectively.

of $\partial W/\partial I_i$ because both the numerator and denominator in eqs 5 and 6 are very small at small deformations.

The reproducibility of the estimated W for the original experimental data is demonstrated in Figures 5 and 6

Table 1. Fractions of Unreacted Reactants, Equilibrium Shear Modulus and Numerical Coefficients in Eq 8 for End-Linked PDMS Networks

polymer concn (wt %)	w_{sol} (wt %)	G_o (Pa)	C_{10} (Pa)	C_{11} (Pa)	C_{01} (Pa)	C_{20} (Pa)	C_{02} (Pa)	C_{11}/C_{10}	C_{01}/C_{10}	C_{20}/C_{10}	C_{02}/C_{10}
100	8.76	1.44×10^5	5.90×10^4	-2.47×10^3	1.32×10^4	1.05×10^3	2.95×10^2	-4.19×10^{-2}	2.24×10^{-1}	1.78×10^{-2}	5.00×10^{-3}
70	7.50	6.49×10^4	2.60×10^4	-1.09×10^3	6.45×10^3	4.42×10^2	1.28×10^2	-4.19×10^{-2}	2.48×10^{-1}	1.70×10^{-2}	4.92×10^{-3}

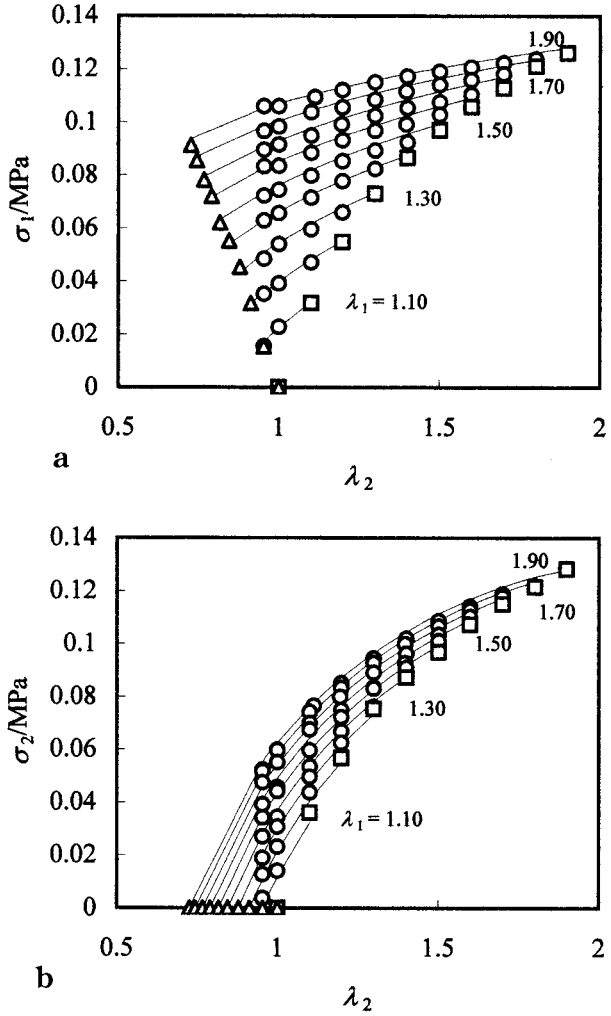

Figure 5. Comparison of the experimental λ_2 dependence of (a) σ_1 and (b) σ_2 with the prediction by the estimated W (solid lines) for the end-linked PDMS network prepared from 70 wt % solution.

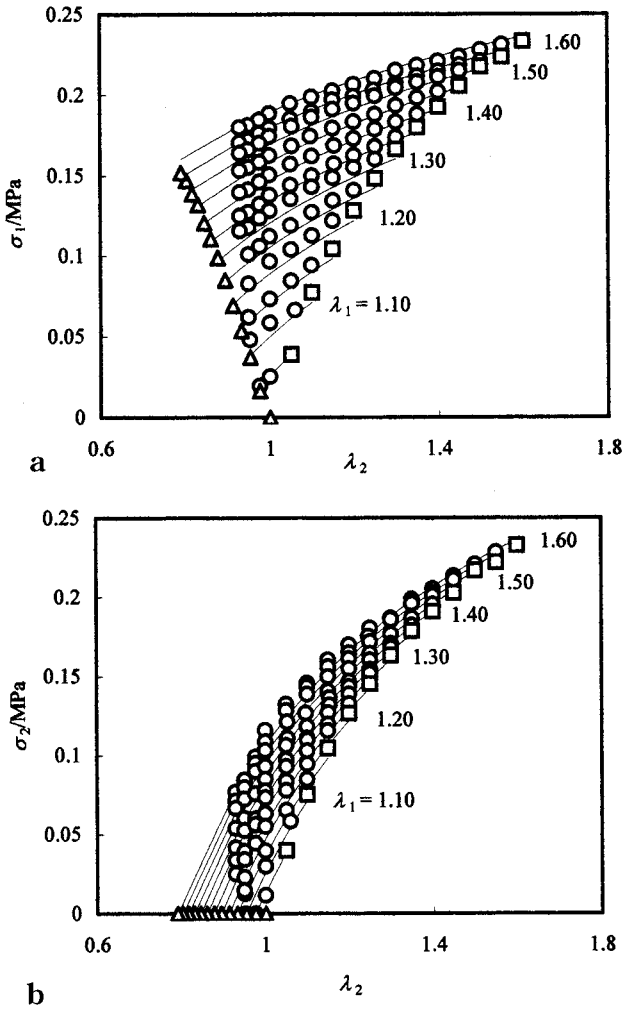

Figure 6. Comparison of the experimental λ_2 dependence of (a) σ_1 and (b) σ_2 with the prediction by the estimated W (solid lines) for the melt-end-linked PDMS network.

for the solution- and melt-end-linked networks, respectively. It is seen for both the networks that the calculated curves by the estimated W (solid lines) successfully reproduce the original biaxial stress−strain data. It is noteworthy that the predictions of the W also quite well agree with the experimental data of the uniaxial and equibiaxial elongation which were not employed for the original estimation of the W. This point will also be discussed in the next section. It is also found in Figures 5 and 6 that the deduced W predicts the stress−strain relations with good accuracy even at the small deformations where the I_i dependence of $\partial W/\partial I_j$ $(i,j = 1,2)$ is not well approximated by the planes. The considerable deviation from eqs 9 and 10 at the small deformations (Figures 3 and 4) is not noticeable in the stress−strain expression.

Tests of the Estimated *W* by Uniaxial Compression and Uniaxial and Equibiaxial Elongation. It is very important to test the reproducibility of the estimated W (eq 8) for experimental stress−strain data under other deformations (i.e., except for biaxial elongation of $\lambda_1 \neq \lambda_2$). In the present study, such attempt was made using uniaxial compression, uniaxial and equibiaxial elongation, none of which were used for the original deduction of eq 8 because eqs 5 and 6 are undefined. Uniaxial compression and equibiaxial elongation are the same "equibiaxial" strain state, but they are different in the stress state. Figure 7 illustrates the comparison of the experimental stress−strain relations and the calculated ones by eq 8 for uniaxial compression, uniaxial and equibiaxial elongation for the two networks. For both the networks, the calculated curves of eq 8 (solid lines) satisfactorily reproduce the experimental data for uniaxial compression as well as uniaxial and equibiaxial elongation. It is to be noted that the W of eq 8 well describes the significant nonlinear stress−strain behavior at large compression and elongation. These results strongly support the validity of the estimated W.

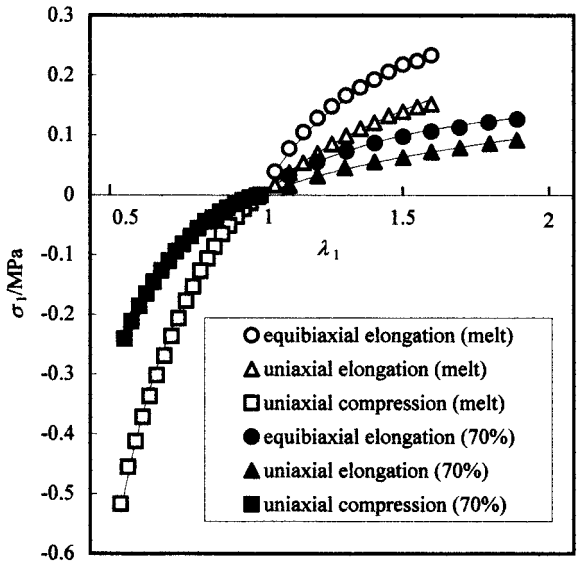

Figure 7. Comparison of the experimental stress−strain relations with the predictions by the estimated W (solid lines) for the end-linked PDMS networks prepared from melt and 70 wt % solution under uniaxial and equibiaxial elongation and uniaxial compression (none of which were employed in the original estimation of W).

Numerical Coefficients C_{ij}. The double of the sum of C_{10} and C_{01} corresponds to the equilibrium shear modulus G_o since G_o is written as[1]

$$G_o = \lim_{I_1,I_2\to 3} 2\left(\frac{\partial W}{\partial I_1} + \frac{\partial W}{\partial I_2}\right) = 2(C_{10} + C_{01}) \qquad (11)$$

The values of G_o calculated from eq 11 are 1.44×10^5 and 6.49×10^4 Pa for the networks prepared from melt and 70 wt % solution, respectively. These values are in very good agreements with $G_o = 1.37 \times 10^5$ Pa and $G_o = 6.48 \times 10^4$ Pa for the melt- and solution-end-linked networks, respectively, estimated from uniaxial elongation measurements in linear elastic region using $E_o = 3G_o$ where E_o is the Young's modulus. The ratio of G_o for the two networks (ca. 0.45) is very close to the square ratio of the effective polymer volume fractions $(0.62/0.92)^2$ where the fractions of unreacted precursor PDMS (w_{sol}) are subtracted. The nearly square dependence of elastic modulus on polymer concentration suggests that the number of the elastic chains is mainly governed by trapped entanglements.[24,25] Also, the magnitude of G_o of the melt-end-linked network is reasonably well explained by the quasi-plateau shear modulus of uncross-linked entangled PDMS melt ($G_N^o = 2.0 \times 10^5$ Pa[36]) together with the consideration of the effective polymer volume fraction: $G_N^o(0.92)^2 \sim 1.6 \times 10^5$ Pa. The slightly smaller value of G_o of the network relative to $G_N^o(0.92)^2$ should be due to a finite amount of dangling chains which do not contribute to equilibrium modulus. These results support the expectation, based on the much higher molecular mass of the precursor PDMS relative to M_c, that trapped entanglement is dominant in number relative to chemical cross-link in the networks used here.

The physical meaning of the higher-order terms is more obscure relative to that of the linear terms. It has been generally considered that the terms except for $(I_1 - 3)$ term originate from entanglement effects which are neglected in the classical rubber elasticity theories.[1,2] This consideration is based on the general trend that the ratio C_{01}/C_{10}, often evaluated from the Mooney−Rivlin plots, decreases with swelling or dilution at preparation.[1,2] However, the physical basis of the higher-order terms has not yet been fully understood and characterized. In the present study, for both the networks, C_{11} is negative, while all other coefficients are positive. The earlier studies[15,37] attempted to employ the expansions of eq 4 up to second or third-order as the W of some rubber vulcanizates: In the most cases the values of C_{11} are negative, while the sign of C_{20} and C_{02} appears to depend on the samples. The signs of the higher-order terms in the present study do not deviate from the general tendencies observed in the earlier studies. With the aid of the Drucker stability criterion, it is easily shown that some negative coefficients are physically admissible if other positive coefficients have appropriate relative magnitudes. The W with the chosen constants must satisfy Drucker's criterion which ensures the physically realistic and stable responses in all deformation states: The internal energy is requested to increase when the material is deformed.[38,39]

$$\sum_i d\sigma_i d\epsilon_i \geq 0 \qquad (12)$$

where $d\sigma_i$ is an increment in the ith principal stress and $d\epsilon_i$ an increment in the corresponding strain. It is easily verified in Figures 5 and 6 that the W functions (eq 8) with the estimated sets of C_{ij} satisfy eq 12: Each of the calculated principal stresses *always* increases with an increase in the corresponding principal strain. It should be emphasized again that the general biaxial elongation experiments as performed here cover all accessible pure homogeneous deformations for an incompressible material.[1,7] Accordingly the confirmation of the Drucker's criterion over the whole range from uniaxial elongation to equibiaxial elongation is sufficient for ensuring the physical stability of the estimated W.

The ratio of the coefficient of each term to C_{10} (C_{ij}/C_{10}), as a measure of the relative contribution of each nonlinear higher order term, is listed in Table 1. Despite the presence of 30 wt % diluent, the contribution of each term for the solution-end-linked network is comparable to that for the melt-end-linked one. This suggests that the 70 wt % solution of the precursor PDMS used here is so concentrated that the elastic contribution of trapped entanglements is still dominant relative to chemical cross-links, although the dilution certainly reduces the number of entanglements (as recognized in decrease in elastic modulus). To elucidate the physical origin of each nonlinear higher-order terms, it will be necessary to investigate the W of the networks prepared from more diluted solution, or the networks in the swollen state. This is a future subject of our study.

Test of the Mooney-Rivlin Type of W. Finally, we demonstrate the inapplicability of the familiar Mooney−Rivlin (M−R) equation to phenomenological strain energy density function, which has also been pointed out in earlier studies.[16,34,40] The M−R equation and "the M−R plot" have often been used due to their simplicity for both phenomenological and molecular interpretations of experimental stress−strain relations.[1,2] The M−R plot,[27,28] the plot of $\sigma_M = \sigma_1/(\lambda_1 - \lambda_1^{-2})$ against λ_1^{-1} for uniaxial deformation data, was proposed as a simple method to obtain the W only from uniaxial deformation measurement on the basis of the "apparent" linearity frequently observed: If the formula of W is

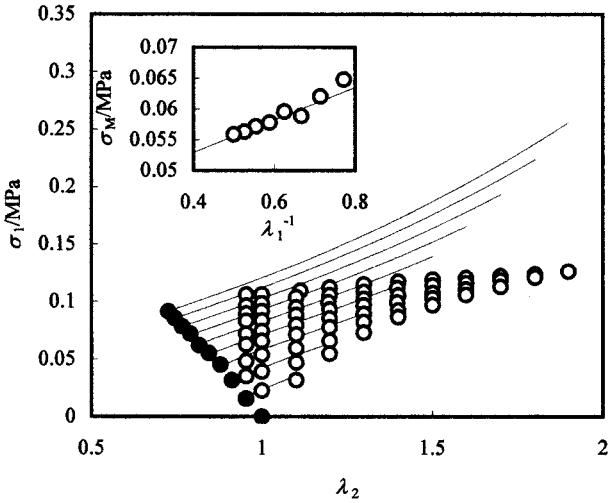

Figure 8. Comparison of the experimental biaxial stress−strain relation with the prediction based on the Mooney−Rivlin type of W for the end-linked PDMS network prepared from 70 wt % solution. The constants C_1 and C_2 in the M−R type of W were obtained from the slope and intercept in the M−R plot ($\sigma_M = \sigma_1/(\lambda_1 - \lambda_1^{-2})$ vs λ_1^{-1}) (shown by the inset) for uniaxial stretching data (closed symbols).

given by the following M−R equation

$$W = C_1(I_1 - 3) + C_2(I_2 - 3) \tag{13}$$

where C_1 and C_2 are constants, uniaxial stretching stress σ_1 is expressed by

$$\sigma_1 = 2\left(\lambda_1 - \frac{1}{\lambda_1^2}\right)\left(\frac{\partial W}{\partial I_1} + \lambda_1^{-1}\frac{\partial W}{\partial I_2}\right) \tag{14}$$

Using eqs 13 and 14, they argued that the slope and intercept of the M−R plot correspond to $2C_2$ and $2C_1$, respectively.[27,28]

In Figure 8, the experimental biaxial stress−strain relation for the solution-end-linked network is compared with the calculated one by eq 13 with the constants C_1 and C_2 which were determined from the M−R plot (the inset of Figure 8) of the uniaxial elongation data. Despite the good linearity of the M−R plot, it is evident that the prediction of the M−R type of W does not even qualitatively agree with the experimental data of biaxial elongation: As a whole, the estimated M−R type of W overestimates the stress, and the predicted sharp upturn of the stress−strain curve for constant λ_1 is far from the real behavior. The inapplicability of the M−R type of W is also easily recognizable from the fact that the experimental $\partial W/\partial I_i$ definitely depends on I_1 and I_2 (as seen in Figures 3 and 4) contrary to the constancy of $\partial W/\partial I_i$ postulated by eq 13, i.e., $\partial W/\partial I_1 = C_1$ and $\partial W/\partial I_2 = C_2$. These results once again show the complete inadmissibility of the M−R type of W in accord with the results in the earlier studies.[16,34,40] Therefore, any effort to estimate the M−R type of W from uniaxial deformation data is not fruitful, and in addition, any attempt to give a molecular interpretation to the empirical parameters obtained from the M−R plots has no definite physical basis.

Summary

The phenomenological strain energy density function W for the elastomeric end-linked PDMS networks, prepared from the melt and concentrated (70 wt %) solution, was deduced as a function of the first and second invariants I_1 and I_2 of the Green's deformation tensor on the basis of the quasi-equilibrium stress−strain relation of biaxial elongation. It was found for both the melt- and solution-end-linked networks that in the large deformation region of $I_1, I_2 > 3.2$, the variation of each of $\partial W/\partial I_1$ and $\partial W/\partial I_2$ on both I_1 and I_2 in the 3-dimensional (I_1,I_2, $\partial W/\partial I_i$) space was well approximated by a plane with a finite gradient against the (I_1,I_2) plane. This suggests that $\partial W/\partial I_i$ ($i = 1,2$) is a linear function of each of I_1 and I_2. The functional form of W was estimated from such linear dependence of $\partial W/\partial I_i$ on I_j ($i,j = 1,2$) as $W = C_{10}(I_1 - 3) + C_{01}(I_2 - 3) + C_{11}(I_1 - 3)(I_2 - 3) + C_{20}(I_1 - 3)^2 + C_{02}(I_2 - 3)^2$. Each of the five coefficients was obtained from each of the intercepts at $I_1 = I_2 = 3$ and the gradients of the two fitted planes. The deduced W was successful in reproducing not only the original biaxial stress−strain data but also the data of other deformations such as uniaxial tension, equibiaxial elongation, and uniaxial compression. The presence of 30 wt % diluent at preparation does not alter the ratios C_{ij}/C_{10}, as a measure of the contribution of each nonlinear higher-order term, as well as the functional form of W. This suggests that the network prepared from 70 wt % solution still possesses elastically entanglement-dominant character similar to the melt-end-linked network.

At the small deformations of $I_1, I_2 < 3.2$, the dependence of each derivative on I_i appears to be different from the plane-approximated dependence at the larger deformations. For the melt-end-linked network, with approaching zero strain limit, $\partial W/\partial I_1$ tends to increase, while $\partial W/\partial I_2$ has a tendency to lessen and become negative. On the other hand, each $\partial W/\partial I_i$ for the solution-end-linked network shows behavior opposite to that for the melt-end-linked network. The puzzling discrepancies in the behavior of the derivatives between the two networks suggest the necessities of further experimental survey in the small deformation region, despite the experimental difficulties of precise estimation of the derivatives at small deformations. However, it is to be noted that the W (eq 8) estimated from large deformation behavior reproduces the stress−strain relations with good accuracy even at the small deformations. In other words, the appreciable deviation from eq 8 at the small deformations observed in the $I_i - \partial W/\partial I_j$ expression is not noticeable in the stress−strain expression. It was also clearly demonstrated that the familiar Mooney−Rivlin function $W = C_1(I_1 - 3) + C_2(I_2 - 3)$, combined with the M−R plot of uniaxial stress−strain data, was not even qualitatively successful in reproducing the experimental biaxial stress−strain data.

Acknowledgment. This work is partly supported by a Grant-in-Aid from the Ministry of Education, Science, Sports, and Culture of Japan (Nos. 09750990 and 12875127).

References and Notes

(1) Treloar, L. R. G. *The Physics of Rubber Elasticity*, 3rd ed.; Oxford University Press: Oxford, England, 1975.
(2) Erman, B.; Mark, J. E. *Structure and Properties of Rubberlike Networks*; Oxford University Press: Oxford, England, 1997.
(3) Seibert, D. J.; Schöche, N. *Rubber Chem. Technol.* **2000**, *73*, 366.
(4) Kaliske, M.; Heinrich, G. *Rubber Chem. Technol.* **1999**, *72*, 602.
(5) Boyce, M. C.; Arruda, E. M. *Rubber Chem. Technol.* **2000**, *73*, 504.

(6) Rivlin, R. S.; Saunders: D. W. *Philos. Trans. R. Soc.* **1951**, *A243*, 251.
(7) Tschoegl, N. W.; Gurer. C. *Macromolecules* **1985**, *18*, 680.
(8) Treloar, L. R. G. *Trans. Faraday Soc.* **1943**, *39*, 36.
(9) Jones, D. F.; Treloar, L. R. G. *J. Phys. D.: Appl. Phys.* **1975**, *8*, 1285.
(10) Vangerko, H.; Treloar, L. R. G. *J. Phys. D.: Appl. Phys.* **1978**, *11*, 1969.
(11) Miguel, A. S.; Landel, R. F. *Trans. Soc. Rheol.* **1966**, *10*, 369.
(12) Glucklich, J.; Landel, R. F. *J. Polym. Sci., Polym. Phys.* **1977**, *15*, 2185.
(13) Tsuge, K.; Arenz, R. J.; Landel, R. F. *Rubber Chem. Technol.* **1978**, *51*, 948.
(14) Becker, G. W. *J. Polym. Sci., Part C* **1967**, *16*, 2893.
(15) James, A. G.; Green, A.; Simpson, G. M. *J. Appl. Polym. Sci.* **1975**, *19*, 2033.
(16) Kawabata, S.; Kawai, H. *Adv. Polym. Sci.* **1977**, *24*, 89.
(17) Kawabata, S.; Matsuda, M.; Tei, K.; Kawai, H. *Macromolecules* **1981**, *14*, 154.
(18) Konkle, G. M.; Selfridge, R.; Servais, P. C. *Ind. Eng. Chem.* **1947**, *39*, 1410.
(19) Urayama, K.; Yokoyama, K.; Kohjiya, S. *Polymer* **2000**, *41*, 3273.
(20) Gottlieb, M.; Macosko, C. W.; Benjamin, K. O.; Mayers, K. O.; Merril, E. W. *Macromolecules* **1981**, *14*, 1039.
(21) Mark, J. E. *Adv. Polym. Sci.* **1982**, *44*, 1.
(22) Xu, P.; Mark, J. E. *Rubber Chem. Technol.* **1990**, *63*, 276.
(23) Patel, S. K.; Malone, C.; Cohen, C.; Gillmor, J. R.; Colby, R. H. *Macromolecules* **1992**, *25*, 5241.
(24) Urayama, K.; Kohjiya, S. *J. Chem. Phys.* **1996**, *104*, 3352; *Eur. Phys. J. B* **1998**, *2*, 75.
(25) Urayama, K.; Kawamura, T.; Kohjiya, S. *J. Chem. Phys.* **1996**, *105*, 4833.
(26) Urayama, K.; Kawamura, T.; Kohjiya, S. Multiaxial Deformations of End-linked Poly(dimethylsiloxane) Networks: 2. Experimental Tests of Molecular Entanglement Models of Rubber Elasticity. *Macromolecules* **2001**, *34*, 8261.
(27) Mooney, M. *J. Appl. Phys.* **1940**, *11*, 582.
(28) Rivlin, R. S. *Philos. Trans. R. Soc. London, A* **1948**, *A241*, 379.
(29) Wang, B.; Krause, S. *Macromolecules* **1987**, *20*, 2201.
(30) Orrah, D. J.; Semlyen, J. A.; Ross-Murphy, S. B. *Polymer* **1988**, *29*, 1452.
(31) Urayama, K.; Takigawa, T.; Masuda, T. *Macromolecules* **1993**, *26*, 3092.
(32) Takigawa, T.; Morino, Y.; Urayama, K.; Masuda, T. *Polym. Gels Networks* **1996**, *4*, 1.
(33) Holownia, B. P. *Rubber Chem. Technol.* **1975**, *48*, 246.
(34) Fukahori, Y.; Seki, W. *Polymer* **1992**, *33*, 502.
(35) Takigawa, T.; Yamasaki, S.; Urayama, K.; Takahashi, M.; Masuda, T. *Rheol. Acta* **1996**, *35*, 288.
(36) Plazek, D. J.; Dannhuser, W.; Ferry, J. D. *J. Colloid Sci.* **1961**, *16*, 101.
(37) Haines, D. W.; Wilson, W. D. *J. Mech. Phys. Solids* **1979**, *27*, 345.
(38) Johnson, A. R.; Quigley, C. J.; Mead, J. L. *Rubber Chem. Technol.* **1994**, *67*, 904.
(39) Yeoh, O. H.; Fleming, P. D. *J. Polym. Sci.: Part B: Polym. Phys.* **1997**, *35*, 1919.
(40) Gottlieb, M.; Gaylord, R. J. *Macromolecules* **1987**, *20*, 130.

MA002165Y